Journal of Engineering and Applied Sciences 15 (2): 421-429, 2020
ISSN: 1816-949X

Production of $KMnO_4$ Loaded Activated Carbon from Sacha Inchi Seed Shell by Low Activation Temperature Treatment for Methylene Blue Removal

[1]Sumrit Mopoung, [2]Russamee Sitthikhankaew and [1]Jenjira Kruekit
[1]Department of Chemistry, Faculty of Science, Naresuan University, Phitsanulok, Thailand
[2]School of Renewable Energy and Smart Grid Tecnology, Naresuan University,
6500 Phitsanulok, Thailand

Abstract: The production of activated carbon from sacha inchi seed shell for methylene blue removal was studied. The effects of $KMnO_4$ impregnation ratios (0-5% wt./wt.) and activation temperature (250-400°C) were evaluated. It was found that the optimum activating temperature and impregnation ratio are 350°C and 1 wt.% $KMnO_4$, respectively. The product made under these conditions is stable and suitable for adsorption in aqueous solution. Maximum methylene blue adsorption was achieved at pH 3 and with a relative decrease to about 95-96% adsorption efficiency between pH 4 and 9. The equilibrium adsorption data showed a good fit with the Freundlich isotherm exhibiting 99.80 mgg^{-1} adsorption capacity.

Key words: Activated carbon, low activation temperature, sacha inchi shell, $KMnO_4$, methylene blue, equilibrium

INTRODUCTION

Regular production of activated carbon is be costly due to the use of high temperature treatment in the production process. Therefore, it is necessary to find suitable conditions for the production of activated carbon using a minimum activation temperature. This will help reduce costs and preserve the environment during activated carbon production. Especially, air activation at low temperature will produce high carbon yield. Moreover, the use of agricultural residues or industrial effluents for activated carbon production will result in further cost reductions. Agricultural waste which is lignocellulosic material is high volume source for the commercial activated carbon production (Ceyhan *et al*., 2013). It contains cellulose, hemicellulose and lignin with a relatively high carbon content that determines the high yield and heterogeneous porosity of the produced activated carbons (Marrakchi *et al*., 2017). Sacha inchi seed shell that is derived from production of sacha inchi seed oil is also one of the potential starting materials for the production of activated carbon. It has been used for fuel gas production by gasification in a drop tube reactor (Lakkhana *et al*., 2017) and the silver nanoparticles synthesis (Wang *et al*., 2018). Surface modification is a way to improve adsorption capacity of activated carbons creating pore structures and functional groups on activated carbon surface. Oxidation modification is the most common method of regulating oxygen-containing functional groups on the activated carbon surface (Zhang *et al*., 2017). Permanganate is a strong oxidizing agent in many organic and inorganic redox reactions and it is also eco-friendly (Das *et al*., 2009). It can significantly improve the content of oxygen-containing surface functional groups of activated carbons (Zhang *et al*., 2017). It has been used for treatment of textile wastewater and soil as it is an easy to handle and a readily soluble solid (Xu *et al*., 2005; Zhang *et al*., 2017). Methylene blue is a cationic dye which has various applications in chemistry, biology, medical science and dyeing industries. Its long term exposure can cause vomiting, nausea, anemia, hypertension (Pathania *et al*., 2017) and also carcinogenesis (Narvekar *et al*., 2018). Further some harmful effects like eye burns, cyanosis, increased heart rate, tachycardia, tissue necrosis, ethemoglobinemia, dyspnea, jaundice and diarrhea in human beings (Ahsaine *et al*., 2018). Furthermore, it can increases the turbidity levels of water, hindering the ability of fish and other organisms to locate food and reducing photosynthetic activity (Spagnoli *et al*., 2017).

In this study, the preparation of activated carbon with one-stage pyrolysis by partial air and $KMnO_4$ oxidation from the sacha inchi seed shell is studied. It is expected that potassium permanganate will reduce the pyrolysis temperature for activated carbon production from lignocellulosic materials. The effects of $KMnO_4$ impregnation ratios (0-5%) and pyrolysis temperature (250-400°C) on final products were investigated. The best product obtained at low pyrolysis temperature was collected for methylene blue adsorption from aqueous solutions.

Corresponding Author: Sumrit Mopoung, Department of Chemistry, Faculty of Science, Naresuan University, Phitsanulok, Thailand

MATERIALS AND METHODS

Preparation of pyrolyzed products: Sacha inchi seed shell was obtained from seed oil production at Wee Organic Co. Ltd., Kamphaeng Phet province of Thailand. It was dried in an oven (SL 1375 SHEL LAB 1350 FX) at 110°C for 3 h. The resulting dried sample was mixed with 0, 1, 3 and 5% $KMnO_4$ by weight. The mixed samples were added to a small amount of distilled water to dissolve $KMnO_4$ to distribute it throughout all the sacha inchi seed shell matter and then dried in an oven under air atmosphere at 105°C for 24 h. The dried mixed samples were then pyrolyzed in closed ceramic crucibles at final temperatures of 250, 350 and 400°C for a holding time of 6 h under partial oxidation conditions in an electric muffle furnace (Fisher Scientific Isotemp® Muffle Furnace). The samples were subsequently cooled to room temperature. The percent yields of pyrolyzed products were measured. The pyrolyzed products were ground, sieved to 50 mesh and then kept in plastic bag for further experiments. BET (Micromeritics TriStar II), SEM-EDS (LEO 1455 VP), FTIR (Spectrum GX, Perkin Elmer) and XRD (XRD, PW 3040/60, X' Pert Pro MPD) were used for characterization of the pyrolyzed products.

Methylene blue adsorption experiment: The effects of different parameters such as contact time, pH and modified activated carbon dosage were investigated. Langmuir and Freundlich isotherm models were also studied from the equilibrium adsorption data with variation of methylene blue concentration.

Equilibrium time of methylene blue adsorption: The 100 mg L^{-1} stock solution of methylene blue was prepared by dissolving 0.1 g of methylene blue powder in 1 L of deionized water.

Batch experiments were used for methylene blue adsorption. The 0.1 g of the non-modified activated carbon or $KMnO_4$ modified activated carbon was added into an erlenmeyer flask containing 25 mL of 10 mg L^{-1} methylene blue solution at pH 7.0±0.15 and then shaken continuously at 120 rpm at a temperature of 32±2°C with contact times of 20, 40, 60, 80, 100, 120, 140, 160 and 180 min. The solutions were then filtered using Whatman No. 42 filter paper to remove the activated carbon particles at the end of each contact time. The absorbance values of the resulting methylene blue filtrates were measured at 665 nm using a UV double beam instrument (Speccord 200 plus). The concentrations of the methylene blue filtrate solutions were calculated from the absorbance values using standard calibration curve. The data from this experiment was graphed to find equilibrium time.

Effect of pH on methylene blue adsorption: In addition to the equilibrium time investigation, an experiment with 60 min contact time for pH of 2, 3, 4, 5, 6, 7, 8 and 9, respectively was carried out. The pH values of solutions were adjusted with 0.05 M HCl or 0.05 NaOH solution. Then methylene blue concentrations in filtrates from all experiments were measured.

Effect of activated carbon dosage on methylene blue adsorption: Like the pH effect experiment, the batch experiments carried out to study of the effect of activated carbon dosage on methylene blue adsorption were carried out with 60 min contact time at pH of 3.0 and 100 mg L^{-1} methylene blue concentration with different doses of activated carbon 0.05, 0.1, 0.5, 1.0, 1.5 and 2.0 g. The methylene blue concentrations in filtrates from each dosage were also measured.

Adsorption isotherms: The data of the effect of activated carbon dosage on methylene blue adsorption experiment were fitted with both the linear form of Langmuir equation (Eq. 1) and Freundlich equation (Eq. 2) (Mopoung *et al*., 2016) as follows: the linear form of Langmuir equation is:

$$C_e/Q_e = 1/(q_{max}K_L)+C_e/q_{max} \quad (1)$$

Where:

- Q_e(mg g^{-1}) : The amount of methylene blue adsorbed per unit mass of activated carbon
- C_e(mg L^{-1}) : The methylene blue equilibrium concentration
- q_{max}(mg g^{-1}) : The maximum methylene blue amount that forms a complete monolayer on the surface of activated carbon
- K_L(L mg^{-1}) : The Langmuir constant related to adsorption heat.
- q_{max} and K_L : Constants can be determined from the slope and intercept of plot of C_e/Q_e against C_e, respectively

The linear form of Freundlich equation is:

$$\log Q_e = \log K_F+1/n \log C_e \quad (2)$$

where, Q_e and C_e have the same definitions as those in the Langmuir equation cited above. K_F and n are Freundlich constants related to adsorption capacity and heterogeneity factor, respectively. The constants K_F and n can be determined from the intercept and slope of plotting log C_e against log Q_e, respectively.

RESULTS AND DISCUSSION

Percent yield of pyrolyzed products: The percent yields of pyrolyzed products made from sacha inchi seed shell without modification and with modification using 1-5% $KMnO_4$ are shown in Table 1. The results show that the

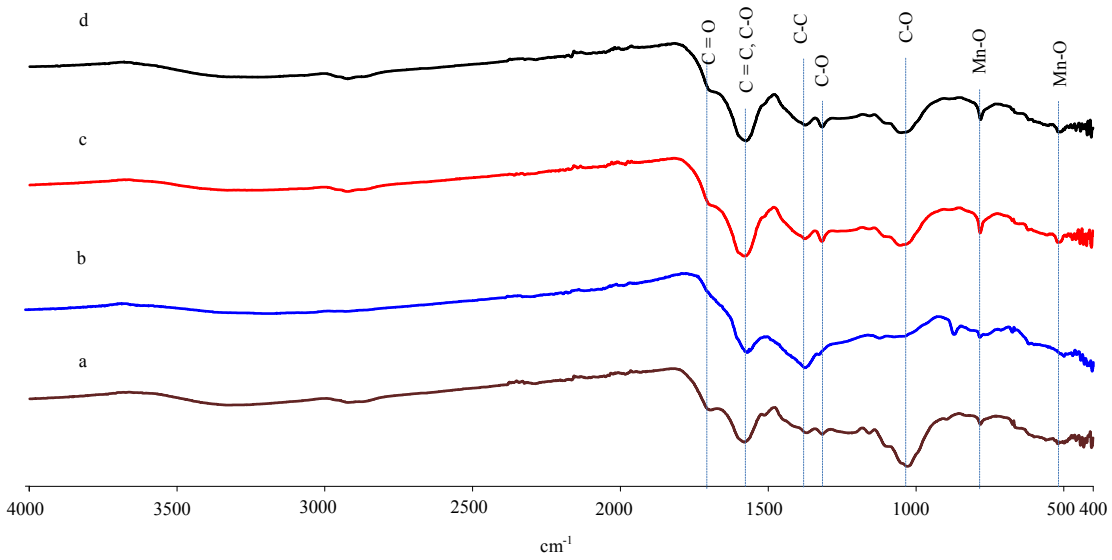

Fig. 1(a-d): Transmission FTIR spectrum of (a) Unmodified (b) 1% $KMnO_4$ modified (c) 3% $KMnO_4$ modified and (d) 5% $KMnO_4$ modified pyrolyzed products prepared at 250°C

Table 1: Percent yield, by dried weight, of pyrolyzed products prepared at 250-400°C without and with 1-5% $KMnO_4$ modification

	Yield at pyrolysis temperature (%)		
Type of pyrolyzed products	250°C	350°C	400°C
Un-modified	38.64	38.57	35.93
1% $KMnO_4$ modified	38.69	35.85	33.76
3% $KMnO_4$ modified	36.82	35.79	33.63
5% $KMnO_4$ modified	35.45	35.15	31.78

percent yield of pyrolyzed products decreases with increasing pyrolysis temperature for the same type of pyrolyzed product. On closer inspection, the percent yield is not different for pyrolysis temperatures in the range of 250-350°C for the same type of pyrolyzed product. However, a more significant decrease is observed at a pyrolysis temperature of 400°C. In addition, the percent yields of pyrolyzed products also relatively decreased with increasing concentration of $KMnO_4$ for the same pyrolysis temperature. Furthermore, when comparing the $KMnO_4$ modified pyrolyzed products to the un-modified one, the percent yield of all $KMnO_4$ modified pyrolyzed products is lower than that of the un-modified one prepared at same pyrolysis temperature. This showes that $KMnO_4$ effects the percent yield of the pyrolyzed products. This observation reveals that the starting materials are degraded by both thermal and $KMnO_4$ oxidation processes. Usually, lignin, hemicellulose, pectin and cellulose are thermally degraded at temperatures between 200 and 350°C (Uner and Bayrak, 2018). The effect of $KMnO_4$ can be due to oxidation of carbon-carbon double bonds of organic matter oxidized by permanganate ion at low pyrolysis temperatures (Das *et al*., 2009).

FTIR spectrum of sacha inchi seed shell and pyrolyzed products: Figure 1 shows transmission FTIR spectra of pyrolyzed products prepared at 250°C. It can be seen that the C = O functional group at 1700 cm^{-1} which is attributed to acetyl groups in the cellulose and hemicellulose structure (Li *et al*., 2016; Usman *et al*., 2015), is still present in the un-modified pyrolyzed product (Fig. 1a). However, its intensity is reduced after $KMnO_4$ modification (Fig. 1b-d). This is because the strong oxidizing agent potassium permanganate reacts with carboxyl groups in the samples (Zhang *et al*., 2017), which are always accompanied by a peak at 1040 cm^{-1} (C-O of glycoside bonds in the polysaccharide structure, lignin, cellulose and hemicellulose) (Kumar *et al*., 2016; Tzvetkov *et al*., 2016). Therefore, the contents of carboxyl C = O and C-O bonds are reduced in the $KMnO_4$ modified products. On the other hand, the peak at 1580 cm^{-1} increased with increasing $KMnO_4$ concentration. This peak is attributed to C = C bond vibrations in aromatic systems and the highly conjugated C-O stretching vibration bands which take place through the growth of aromatic structures and polymerization during the pyrolysis and modification as a result of removal of some volatile matter (Qambrani *et al*., 2017). This phenomenon results in increasing single bond character of C = O groups, which are conjugated to aromatic rings. Likely, the peaks at 1380, 1320 and 1040 cm^{-1} can be assigned C-C stretching in rings and C-O stretching vibration (Feng *et al*., 2018). This shows that an aromatic system is incipient. Additionally, the oxygen-containing functional groups of pyrolyzed $KMnO_4$ modified products also increased. Similarly, the

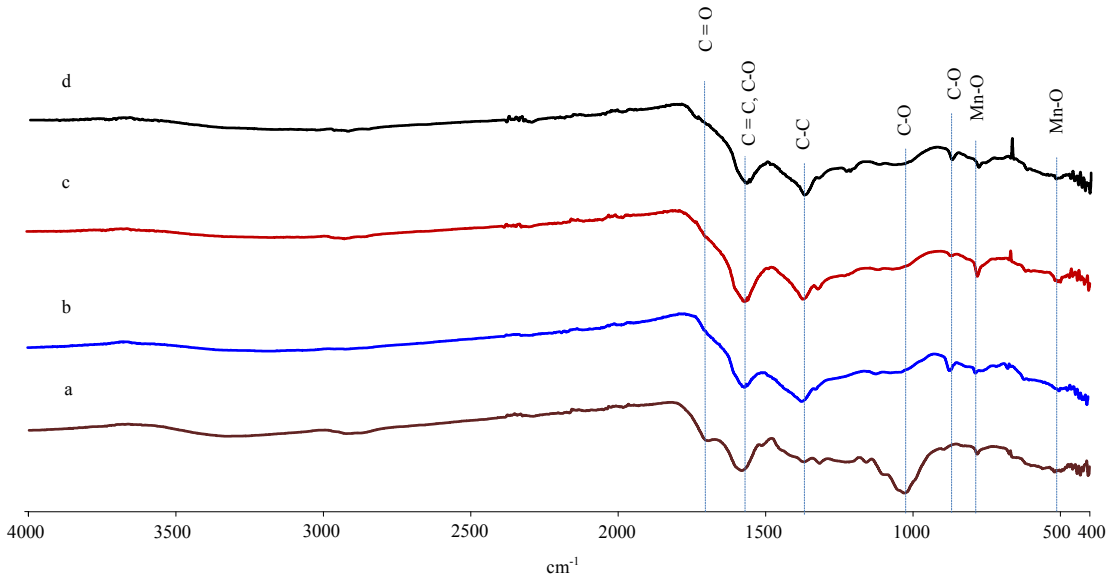

Fig. 2(a-d): Transmission FTIR spectrum of (a) Un-modified product at 250°C and 1% $KMnO_4$ modified pyrolyzed products at 250°C (b), 350°C (c) and 400°C (d)

very small peaks around 780 and 520 cm^{-1} which are present after $KMnO_4$ modification and pyrolysis at 250°C (Fig. 1b-d) are assigned to Mn-O bonds of the Mn oxide phase (Najafpour *et al*., 2016). Moreover, it was noticed that the peaks at 1580, 1380 1320 and 1040 cm^{-1} of pyrolyzed product decreased after modification with 1 wt.% $KMnO_4$ but slightly increased on increasing the wt.% $KMnO_4$ to 3-5%. This indicates that while some of the functional groups of organic matter were degraded with $KMnO_4$ other oxygen-containing function groups have been installed with oxidation using $KMnO_4$. Therefore, these peaks show increased intensity with increasing of wt.% $KMnO_4$.

The effects of pyrolysis temperature on un-modified and 1 wt.% $KMnO_4$ modified products can be seen in Fig. 2. The figure it was clearly shows that the peaks at 1700 cm^{-1} (C = O) and 1040 cm^{-1} (C-O) of un-modified product prepared at 250°C (Fig. 2a) disappeared after 1 wt.% $KMnO_4$ modification at 250-400°C (Fig. 2b-d). Furthermore, it can be seen that the FTIR spectra of products pyrolyzed with 1 wt.% $KMnO_4$ modification products at 250-400°C are similar. Additionally, the peaks at about 1580 and 1380 cm^{-1} which refer to C = C and C-C, respectively, increased after modification with 1% $KMnO_4$ and pyrolysis at 250-400°C. This is because the aromatic character of the products is augmented with condensation reactions induced under these conditions (Xi *et al*., 2018). It points out that the pyrolysis temperature of only 250°C is sufficient to significantly break down the organic matter present in the starting material. These results suggests that products made with pyrolysis using 1 wt.% $KMnO_4$ modification will be sufficiency stable for adsorption applications in aqueous solution.

XRD analysis: Figure 3 shows the XRD spectra of both the un-modified product and product modified with 1% $KMnO_4$ prepared by pyrolysis at 350°C. The spectra indicate presence of amorphous carbon with limited crystal structure. It can be seen that the products made with 1% $KMnO_4$ modification exhibit more characteristics amorphous carbon. Furthermore, it can be seen that some lignin and cellulose are retained in the un-modified product at 350°C (Fig. 3a). However, after modification with 1% $KMnO_4$, the pyrolyzed product shows more MnO_2, K_2O and disordered graphite, while the structured organic compounds have disappeared (Fig. 3b). This indicates that the carbon matrix of the modified pyrolyzed product has been destroyed in the process of oxidation-reduction (Feng *et al*., 2018). However, the diffraction peaks of MnO_2 and K_2O are of low intensity. This because the pyrolyzed modified product was modified with only 1 wt.% of $KMnO_4$ which could not be detected at this low concentration (Zhang *et al*., 2012).

SEM and EDS results of pyrolyzed products: The SEM image of un-modified pyrolyzed products prepared at 350°C shows uniformly distributed knots on its surface (Fig. 4a-b). However, the 1 wt.% $KMnO_4$ modified pyrolyzed product (Fig. 4c-d) is more destroyed in comparison to the un-modified pyrolyzed product. Additionally, the EDS results also showed that the C, Mn and K contents of modified pyrolyzed product have increased (Table 2). This confirms that the charcoal nature of the modified pyrolyzed product has also increased. This result is in agreement with the FTIR and XRD results.

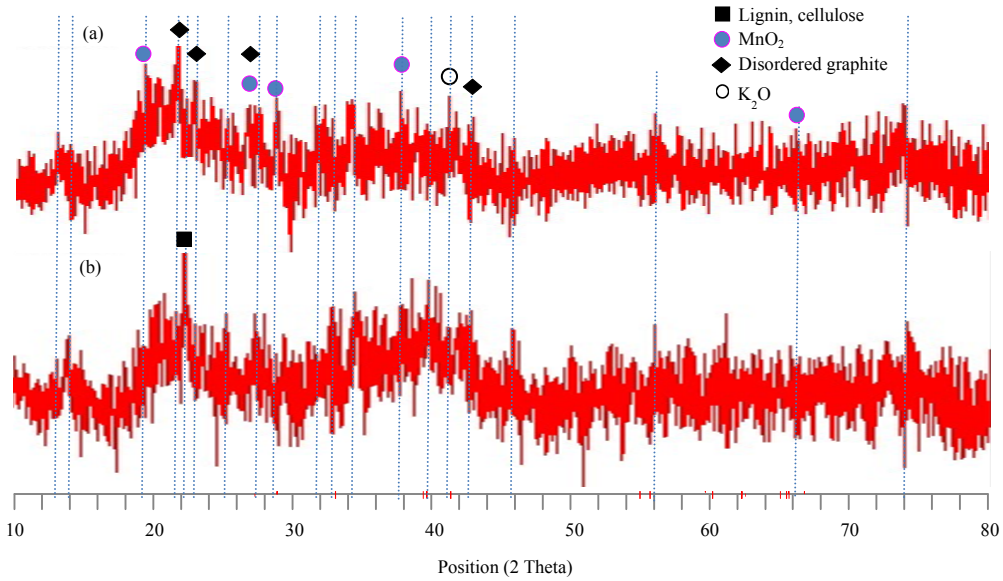

Fig. 3(a-b): XRD spectrum of (a) Un-modified product produced at 350°C (b) 1% $KMnO_4$ modified product prepared by pyrolysis at 350°C

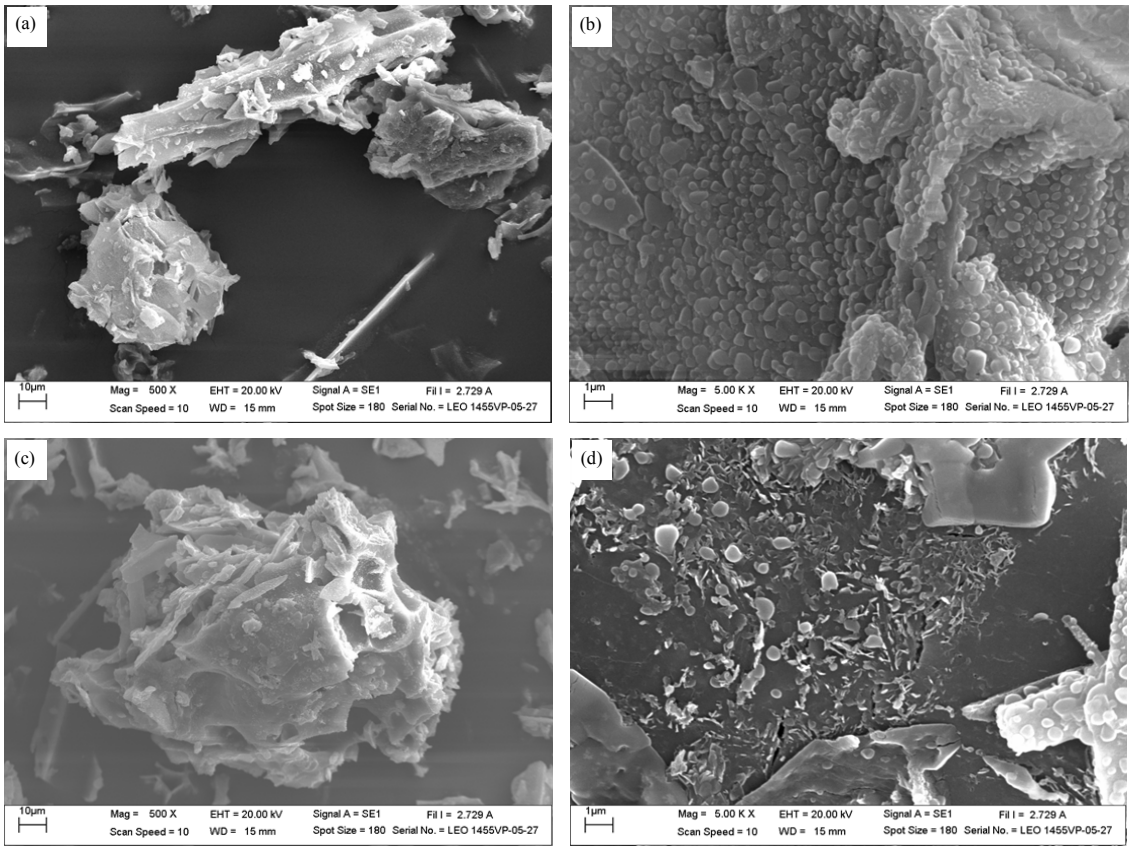

Fig. 4(a-d): SEM micrographs of (a-b) Un-modified product prepared at 350°C and (c-d) 1% $KMnO_4$ modified products prepared by pyrolysis at 350°C

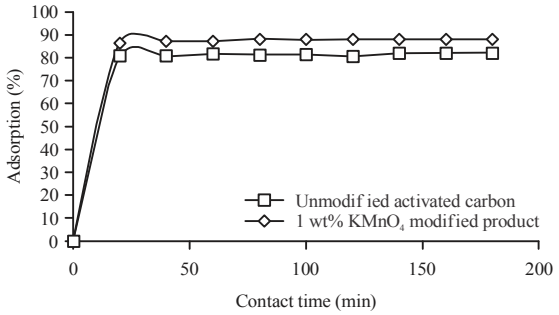

Fig. 5: Equilibrium time for methylene blue adsorption at pH7 on unmodified activated carbon and 1 wt.% $KMnO_4$ modified product prepared at 350°C

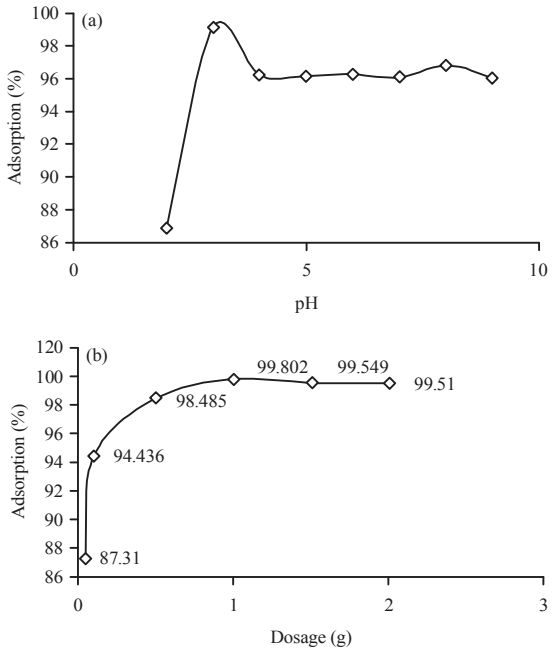

Fig. 6(a-b): (a) Effect of pH 2-9 and (b) Dosage at pH 7 on the efficiency of methylene blue adsorption by 1 wt.% $KMnO_4$ modified product prepared by pyrolysis at 350°C with contact time of 60 min

Table 2: Elemental composition of pyrolyzed products prepared at 350°C by EDS

	Elements (wt.%)			
Samples	C	O	Mn	K
Un-modified product	60.91	32.73	0.87	4.97
1 wt.% $KMnO_4$ modified product	61.34	32.85	2.51	6.15

Methylene blue adsorption

Contact time of methylene blue adsorption: Figure 5 shows the contact times (0-180 min) for 10 mg L^{-1} methylene blue adsorption at pH 7 with activated carbon made with 1 wt.% $KMnO_4$ modification by pyrolysis at 350°C. It can be seen that the absorption equilibrium was reached within only 20 min with about 87% adsorption efficiency. At the same time, the methylene blue adsorption equilibrium of un-modified activated carbon is also achieved at 20 min with about 82% adsorption efficiency (Fig. 5). The relatively short time needed to reach equilibrium may be associated with the high initial content of vacant sites on the surface of activated carbon. Therefore, methylene blue could easily access the active sites of the activated carbon with short contact time. Furthermore, it is clear that the methylene blue adsorption efficiency of modified activated carbon is higher than that of the unmodified activated carbon due both to adsorption and the redox activity of MnO_2 (Dassanayake *et al*., 2016). This has indicated that the modification with $KMnO_4$ is effective. This is attributed to the mesopore structure of the modified activated carbon and the increased number of oxygen containing functional groups after $KMnO_4$ oxidation modification (Feng *et al*., 2018). Thus, the 1 wt.% $KMnO_4$ modified activated carbon prepared by pyrolysis at 350°C was selected for the next experiment with 60 min equilibrium time to assure that the adsorption equilibrium is reached.

Effect of pH on methylene blue adsorption: The pH effect on methylene blue adsorption was observed with 0.1 g of 1 wt.% $KMnO_4$ modified activated carbon prepared by pyrolysis at 350°C in the range pH 2-9 with 25 mL of 10 mg L^{-1} methylene blue solution and 60 min contact time. It experiment has shown that the maximum methylene blue adsorption was achieved at pH 3 (Fig. 6a). At pH values above 3, the % methylene blue adsorption decreased to about 95-96 % adsorption efficiency between pH 4 and 9. These observations could be explained by the effect of ionization and oxidation. At pH values below 3 there is a competition between the hydrogen ions and the cationic dye methylene blue as well as repulsive forces between the positively-charged modified activated carbon surface and methylene blue (Dassanayake *et al*., 2016). Therefore, methylene blue adsorption on modified activated carbon surface is low. At pH 3, the maximum adsorption occurs. This is becaus both adsorption and the oxidative degradation of methylene blue by MnO_2 (Dassanayake *et al*., 2016) on the modified activated carbon are taking place. However, it is expected that the oxidative degradation of methylene blue by MnO_2 is dominant at pH 3. However, at pH values above 3 the oxidizing ability of MnO_2 could be decreased as has been reported by Wang *et al*. (2014). At pH 4-9, deprotonation of the hydroxyl groups on modified activated carbon generates more negatively-charged adsorption sites for the adsorption of the cationic dye methylene blue onto the modified activated carbon (Dassanayake *et al*., 2016). In this pH range, the effect of the adsorption by the ionization process of both the modified activated carbon and methylene blue is dominant.

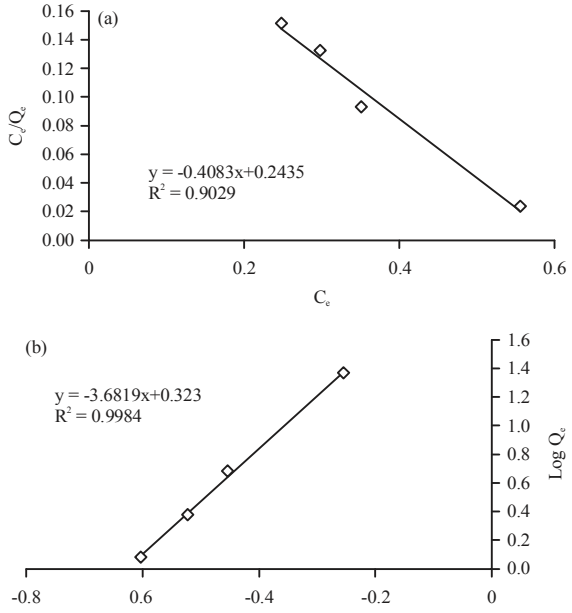

Fig. 7(a-b): Langmuir isotherm (a) and Freundlich isotherm (b) of methylene blue adsorption by 1 wt.% $KMnO_4$ modified product prepared by pyrolysis at 350°C at pH 3 and 60 min contact time

Dosage effect on methylene blue adsorption: The dosage effect experiment on methylene blue adsorption by 1 wt% $KMnO_4$ modified product prepared by pyrolysis at 350°C was investigated by dosage variation using 0.05, 0.1, 0.5, 1.0, 1.5, 2.0 g in 25 mL of 100 mg L^{-1} methylene blue at pH 3 and 60 min contact time. It was seen that the percent adsorption of methylene blue by the modified product increased with increasing of dosage (Fig. 6b). Because of the total adsorption active sites available to methylene blue molecules increased with increasing the modified activated carbon dosage (Pang *et al*., 2017). The maximum adsorption is reached at a dose of 1.0 g and remains relatively constant with increased doses. The calculation of adsorption capacity of methylene blue indicates that was adsorbed with a capacity of 99.80 mg g^{-1} by the 1 wt% $KMnO_4$ modified product prepared by pyrolysis at 350°C.

Isotherm model for methylene blue adsorption: The equilibrium adsorption data from dosage effect experiments were fitted to the Langmuir and Freundlich Model. It was found that the Freundlich isotherm fits to the equilibrium adsorption data with R^2 = 0.9984. This indicated that methylene blue is adsorbed by heterogeneous surfaces of $KMnO_4$ modified product which is increased with increasing methylene blue concentration (Araujo *et al*., 2018). It also shows multilayer adsorption with non-uniform distribution of adsorption heat and affinities (Nitzsche *et al*., 2019). The values of K_F and n parameters are 210.3778 mg g^{-1} (L $mg^{-1})^{1/n}$ and 0.2716, respectively. The Freundlich parameter n for methylene blue adsorption on the modified product is in the range between 0 and 10, indicating favorable adsorption (Nitzsche *et al*., 2019). In addition, the calculated K_F value for methylene blue adsorption on the surface of the modified product is quite high. This indicates that $KMnO_4$ modified activated carbon from sacha inchi seed shell could adsorb methylene blue with high capacity (Fig. 7).

CONCLUSION

In this study, it was shown that $KMnO_4$ could reduce activation temperature and increased methylene blue adsorption for activated carbon prepared from sacha inchi seed shell, in comparison to un-modified product. The percent yields of $KMnO_4$ activated products (31.78-38.64%) decreased with increasing pyrolysis temperature and also decreased with increasing concentration of $KMnO_4$. The results from FTIR, XRD and SEM-EDX showed that the $KMnO_4$ modified product had high content of the oxygen-containing functional groups, MnO_2 and high amorphous carbon character, which make it stable for adsorption using in aqueous solutions. The results have also shown that the optimum activation temperature and impregnation ratio for activated preparation from sacha inchi seed shell are 350°C and 1 wt.% $KMnO_4$, respectively. Methylene blue adsorption experiments have indicated that maximum adsorption is observed at pH 3 and decreases to about 95-96% adsorption efficiency between pH 4 and 9 with a 99.80 mg g^{-1} adsorption capacity. The methylene blue adsorption equilibrium data for 1 wt.% $KMnO_4$ modified activated carbon prepared by pyrolysis at 350°C fits well to the Freundlich isotherm. This shows that methylene adsorption capacity increases with increasing methylene blue concentration. Therefore, the $KMnO_4$ modified activated carbon made from sacha inchi seed shell at low activation temperature can be made by a simple procedure with low cost and shows good ability for methylene blue removal from aqueous solution.

ACKNOWLEDGEMENT

The researchers acknowledge Science Lab Center, Faculty of Science, Naresuan University for all of the analyses.

REFERENCES

Ahsaine, H.A., M. Zbair, Z. Anfar, Y. Naciri and R. El Haouti, *et al*., 2018. Cationic dyes adsorption onto high surface area almond shell' activated Carbon: Kinetics, equilibrium isotherms and surface statistical modeling. Mater. Today Chem., 8: 121-132.

Araujo, C.S.T., I.L.S. Almeida, H.C. Rezende, S.M.L.O. Marcionilio and J.J. Leon *et al*., 2018. Elucidation of mechanism involved in adsorption of Pb (II) onto lobeira fruit (*Solanum lycocarpum*) using Langmuir, Freundlich and Temkin isotherms. Microchem. J., 137: 348-354.

Ceyhan, A.A., O. Sahin, C. Saka and A. Yalcın, 2013. A novel thermal process for activated carbon production from the vetch biomass with air at low temperature by two-stage procedure. J. Anal. Appl. Pyrolysis, 104: 170-175.

Das, S., S. Patel and B.K. Mishra, 2009. Oxidation by permanganate: Synthetic and mechanistic aspects. Tetrahedron, 65: 707-739.

Dassanayake, R.S., E. Rajakaruna, H. Moussa and N. Abidi, 2016. One-pot synthesis of MnO_2-chitin hybrids for effective removal of Methylene blue. Intl. J. Boil. Macromol., 93: 350-358.

Feng, N.C., W. Fan, M.l. Zhu and X.Y. Guo, 2018. Adsorption of Cd^{2+} in aqueous solutions using $KMnO_4$-modified activated carbon derived from Astragalus residue. Trans. Nonferrous Met. Soc. China, 28: 794-801.

Kumar, B., K. Smita, E. Sanchez, C. Stael and L. Cumbal, 2016. Andean Sacha inchi (*Plukenetia volubilis* L.) shell biomass as new biosorbents for Pb^{2+} and Cu^{2+} ions. Ecol. Eng., 93: 152-158.

Lakkhana, C., D. Atong and V. Sricharoenchaikul, 2017. Fuel gas generation from gasification of Sacha inchi shell using a drop tube reactor. Energy Procedia, 138: 870-876.

Li, J., Y. Ren, S. Wang, Z. Ren and J. Yu, 2016. Transition metal doped MnO_2 nanosheets grown on internal surface of macroporous carbon for supercapacitors and oxygen reduction reaction electrocatalysts. Appl. Mater. Today, 3: 63-72.

Marrakchi, F., M.J. Ahmed, W.A. Khanday, M. Asif and B.H. Hameed, 2017. Mesoporous-activated carbon prepared from Chitosan flakes via single-step Sodium hydroxide activation for the adsorption of Methylene blue. Intl. J. Boil. Macromol., 98: 233-239.

Mopoung, S., P. Amornsakchai and S. Somroop, 2016. Characterization of phosphoric acid modified activated carbon fiber from fiber waste of pineapple leaf fiber production processing. Carbon-Sci. Technol., 8: 1-12.

Najafpour, M.M., F. Ebrahimi and M. Holynska, 2016. Nanolayered Mn oxide obtained in the reaction of $KMnO_4$ and Mn2CO10: Conflict between extremes toward an efficient water-oxidizing catalyst. Intl. J. Hydrogen Energy, 41: 2583-2591.

Narvekar, A.A., J.B. Fernandes and S.G. Tilve, 2018. Adsorption behavior of Methylene blue on glycerol based Carbon materials. J. Environ. Chem. Eng., 6: 1714-1725.

Nitzsche, R., A. Groengroeft and M. Kraume, 2019. Separation of lignin from beech wood hydrolysate using polymeric resins and zeolites-determination and application of adsorption isotherms. Sep. Purif. Technol., 209: 491-502.

Pang, J., F. Fu, Z. Ding, J. Lu, N. Li and B. Tang, 2017. Adsorption behaviors of methylene blue from aqueous solution on mesoporous birnessite. J. Taiwan Inst. Chem. Eng., 77: 168-176.

Pathania, D., S. Sharma and P. Singh, 2017. Removal of Methylene blue by adsorption onto activated carbon developed from *Ficus carica* bast. Arabian J. Chem., 10: S1445-S1451.

Qambrani, N.A., M.M. Rahman, S. Won, S. Shim and C. Ra, 2017. Biochar properties and eco-friendly applications for climate change mitigation, waste management and wastewater treatment: A review. Renewable Sustain. Energy Rev., 79: 255-273.

Spagnoli, A.A., D.A. Giannakoudakis and S. Bashkova, 2017. Adsorption of Methylene blue on Cashew nut shell based Carbons activated with Zinc chloride: The role of surface and structural parameters. J. Mol. Liq., 229: 465-471.

Tzvetkov, G., S. Mihaylova, K. Stoitchkova, P. Tzvetkov and T. Spassov, 2016. Mechanochemical and chemical activation of lignocellulosic material to prepare powdered activated Carbons for adsorption applications. Powder Technol., 299: 41-50.

Uner, O. and Y. Bayrak, 2018. The effect of carbonization temperature, carbonization time and impregnation ratio on the properties of activated carbon produced from *Arundo donax*. Microporous Mater., 268: 225-234.

Usman, A.R., A. Abduljabbar, M. Vithanage, Y.S. Ok and M. Ahmad *et al*., 2015. Biochar production from date palm waste: Charring temperature induced changes in composition and surface chemistry. J. Anal. Applied Pyrolys., 115: 392-400.

Wang, M., H. Liu, Z.H. Huang and F. Kang, 2014. Activated Carbon fibers loaded with MnO_2 for removing NO at room temperature. Chem. Eng. J., 256: 101-106.

Wang, S., F. Zhu and Y. Kakuda, 2018. Sacha inchi (*Plukenetia volubilis* L.): Nutritional composition, biological activity and uses. Food Chem., 265: 316-328.

Xi, Y., D. Yang, X. Qiu, H. Wang and J. Huang *et al*., 2018. Renewable lignin-based Carbon with a remarkable electrochemical performance from Potassium compound activation. Ind. Crops Prod., 124: 747-754.

Xu, X.R., H.B. Li, W.H. Wang and J.D. Gu, 2005. Decolorization of dyes and textile wastewater by Potassium permanganate. Chemosphere, 59: 893-898.

Zhang, G., Y. Sun, P., Zhao, Y. Xu, A. Su and J. Qu, 2017. Characteristics of activated carbon modified with alkaline $KMnO_4$ and its performance in catalytic reforming of greenhouse gases CO_2/CH_4. J. CO_2 Util., 20: 129-140.

Zhang, H., J. Chen, P. Liang and L. Wang, 2012. Mercury oxidation and adsorption characteristics of potassium permanganate modified lignite semi-coke. J. Environ. Sci., 24: 2083-2090.